

Experimental Validation of a Computational Fluid Dynamics Model for IAQ applications in Ice Rink Arenas

Chunxin Yang¹, Philip Demokritou^{2*}, Qingyan Chen¹ and John Spengler²

¹Building Technology Program, Department of Architecture,
Massachusetts Institute of Technology, MIT Room 5-418, 77 Massachusetts Avenue,
Cambridge, MA 02139, USA. Fax: (617) 253-6152

²Environmental Science and Engineering Program, School of Public Health,
Harvard University. SPH1-B23, 665 Huntington Avenue,
Boston, MA 02115, USA, Fax: 617-432-4122,

Abstract

Many ice rink arenas have ice resurfacing equipment that uses fossil fuel as power. The combustion byproducts are a major source of contamination. Ventilation along with other pollution source control measures is the most widely applied strategy to lower the contaminant level below the threshold limit and maintain acceptable indoor air quality. A computational fluid dynamics (CFD) model has been used to predict the contaminant concentrations, air velocity, and air temperature distributions in ice rinks. The numerical results agree reasonably with the corresponding experimental data for both steady state and transient conditions. The CFD model is a useful and inexpensive tool to investigate ventilation parameters, such as air distribution methods, ventilation effectiveness, air exchange rates, and various ventilation control strategies.

Keywords: Indoor Air Quality, Ice Rink, Numerical Simulation, CFD

Practical Implications:

Compromised indoor air quality in ice skating arenas due to the combustion byproducts from the fossil powered resurfacing equipment, poses a health risk for both athletes and spectators. Advanced computational fluid dynamics (CFD) modeling can be used effectively to predict the indoor environmental quality in such a unique built environment. A CFD model was developed and validated experimentally for both steady state and transient conditions and used to evaluate IAQ in ice rink arenas. The results show that the CFD model is sufficiently good to predict the air velocity, air temperature, and contaminant concentrations in ice rink arenas.

INTRODUCTION

There are thousands of ice rink arenas worldwide, and many cases with compromised indoor air quality have been reported in such a building environment. A major source of air pollution is the combustion byproducts emitted from the fossil fuel resurfacing equipment. The pollutants include hydrocarbons (HC), carbon monoxide (CO), and NO_x. In many studies, CO and NO_x concentrations in ice rink arenas have been measured up to 100 times as high as usual urban air concentrations (Spengler et al. 1978; Lee et al. 1994; Brauer and Spengler 1994) imposing serious health risks to both spectators and athletes.

Characterizing the contaminant distribution in such a large open space is considered a difficult technical task, taking into consideration the non-uniformity of the indoor air flow created by local heat sources, geometrical obstructions and the air distribution method. The sensitivity of concentration to various flow non-uniformity is identified in many studies (Hangstrom et al,

1999). Therefore, a significant number of data points is required in order to get a reliable contaminant spatial distribution in the space

Two popular approaches are available to determine the distribution of indoor air quality and airflow in such a built environment: experimental measurements and numerical simulation. The experimental approach uses tracer gas methods to study the contamination dispersal and ventilation effectiveness. One example of such an application for ice rink arenas is by Demokritou et al. (1999). The numerical simulation applies the computational fluid dynamics (CFD) technique to study airflow and IAQ in buildings with a turbulence model (Chen 1997). Despite the fact that numerical simulation has been used extensively in studying airflow and IAQ in buildings to the knowledge of the authors, there has no utilization of CFD for ice rink arenas.

The drawback of the experimental methods is the time and the complicated equipment needed for the measurements. A CFD model, on the other hand, can be a powerful tool not only to characterize the existing conditions but also to modify scenarios related to the ventilation system.

In the present study, a CFD model has been developed and validated for both steady-state and transient conditions. The distributions of air velocity, air temperature, CO concentration, and tracer gas concentration measured in an ice rink are used to validate the numerical results. The results have demonstrated that the CFD model can be used with good accuracy to analyze and design such a complicated indoor air environment.

NUMERICAL SIMULATION

The CFD model

The CFD model consists of the conservation equations of mass, momentum, energy, and species concentrations that govern the transport phenomena in ice rinks. The CFD approach numerically solves these equations together with the corresponding boundary conditions for airflow, temperature, and species concentration in ice rink.

Most airflows in buildings are turbulent. With an eddy-viscosity turbulence model, the airflow, temperature, and species transport phenomena can be described by the following time-averaged Navier-Stokes equations:

$$\frac{\partial(\rho\Phi)}{\partial t} + \text{div}(\rho V\Phi - \Gamma_{\Phi, \text{eff}} \cdot \text{grad}\Phi) = S_{\Phi} \quad (1)$$

Where:

- ρ = Air density, kg/m³
- Φ = 1 for mass continuity;
- = V_j (j=1, 2, 3) for three components of momentum;
- = k for turbulent energy;
- = ε for the dissipation rate of k;
- = T for energy transport equation;

- C_i = containment concentrations;
- τ = age of air;
- \mathbf{V} = velocity vector
- $\Gamma_{\Phi, \text{eff}}$ = effective diffusion coefficient
- S_{Φ} = source term

The effective diffusion coefficient and source term for the differential equations are listed in Table 1. The effective viscosity, μ_{eff} , is the sum of molecular viscosity, μ , and turbulent viscosity, μ_t :

$$\mu_{\text{eff}} = \mu + \mu_t \quad (2)$$

where μ is a fluid property while μ_t depends on flow conditions. The effective diffusivity for mass transfer of contamination is:

$$D_{\text{eff}} = \mu / (\rho Sc) + \mu_t / (\rho Sc_t) \quad (3)$$

where Sc and Sc_t are the molecular and turbulent Schmidt numbers for the species.

The CFD model uses approximations in calculating the turbulence quantities, such as isotropic turbulence and the Buossinesq eddy viscosity concept. Chen (1997) has detailed the pros and cons as well as the limitation of the CFD model.

Boundary conditions

The governing equations can be closed with appropriate boundary conditions at all the boundaries such as air inlets, outlets and wall surfaces. The values of velocity, temperature, kinetic energy and its dissipation rate and species concentration should be set at the boundaries.

External walls and obstructions:

A non-slip condition at all solid walls is applied to the velocities. The logarithmic law or wall function has been used (Launder and Spalding, 1974) for the near wall boundary layer because the turbulence model does not work for the low Reynolds number flow near a wall. The present study uses the measured temperatures of the wall and ice surface from the survey as the boundary values for each arena.

Air Inlets:

The measured air temperature, airflow rate, concentration levels at every inlet constitute the corresponding boundary conditions. Velocity, kinetic energy, and its dissipation are estimated as follows:

$$U_{\text{in}} = \frac{M}{\rho A} \quad (4)$$

$$k_{\text{in}} = 0.05 U_{\text{in}}^2 \quad (5)$$

$$\varepsilon_{\text{in}} = 0.09 k_{\text{in}}^{1.5} / D \quad (6)$$

Where

k_{in} = kinetic energy, m^2/s^2 ;

ε_{in} = dissipate rate of kinetic energy, m^2/s^3 ;
 U_{in} = inlet air velocity, m/s;
D = characteristic scale of inlet, m.
M = air flow rate (kg/s)

Steady-state and transient conditions:

The simulations have been performed for both steady-state and transient conditions. Under the steady-state conditions, the ventilation system is assumed on all the time and the pollution source from an ice resurfacer is uniformly distributed on the ice surface. In order to evaluate the CO emissions from the ice resurfacer, the CO emissions were measured for the propane fueled resurfacer and found to be 200mg/s. This CO emission level is typical for an ice resurfacer and was verified in many other similar propane type resurfacers, investigated in our survey.

The emphasis of steady-state simulation is placed on the prediction of air velocity, temperature and contaminant profile in the arena. The CO should be considered as a normalized contaminant source. Normalized means the value presented is normalized by the source strength. This study does not consider any sink effects for the air contaminant. Concentrations of other gaseous pollutants such as NO_x and HC can be calculated by scaling, even though they have a different molecular weights than CO. This was possible because the magnitude of the pollution sources was small and the resulting concentrations were so low as to have a negligible effect on the density of the mixture of air and pollutants.

The transient condition has been used to investigate the dynamic contamination dispersal in an ice resurfacing cycle. Under transient conditions, the basic assumption is that the resurfacer moves in circles around the ice surface for a certain period of time while the ventilation system is on all the time. In order to simulate the circular motion of the ice resurfacer, a number of contamination sources have been distributed over the ice surface. The contamination sources are activated sequentially for a brief period of time to simulate the movement of the resurfacer. Therefore, the boundary condition for the contaminant source was a moving one. The activation time of each source is determined by the moving speed of the resurfacer and the distance between two successively active sources.

Initial conditions for transient conditions

The initial values must also be set for all the variables in the simulation of transient conditions. The investigation uses the steady-state solutions as the initial conditions for pressure, velocity, energy, kinetic energy, and its dissipation rate. However, the initial condition for CO concentration is assumed to be zero.

Numerical procedure

A CFD program, PHOENICS 3.1 (CHAM, 1998), was used to solve the time-dependent conservation equations together with the standard k- ε model (Launder and Spalding, 1974) and the corresponding boundary conditions. The program divided the space of the ice rink into non-uniform computational cells, and the discrete equations were solved with the SIMPLE algorithm (Patankar, 1980). The convergence criteria used at each time step ensured that the total normalized residuals were less than 1% for flow and 3% for CO concentration.

VALIDATION EXPERIMENTS – CASE STUDIES

Air velocity and temperature distribution under steady state conditions:

In this case, numerical simulations and validation tests have been conducted to verify the ability of CFD to predict air velocity and temperature distributions in an arena located in the Boston area. Figure 1 shows the configuration of the ventilation system and the building geometry of the arena. Fresh air is supplied from a side wall through an inlet and is exhausted from four outlets on the opposite wall. The size of the inlet and outlets is 3.6 m by 1.2m and 0.9m by 0.9m, respectively. The air velocity and temperature profiles in front of the inlet were measured and used as boundary conditions in the simulations.

The air velocity and temperature vertical profiles were also measured at six locations, as shown on Figure 1. At each location, air velocity and temperature were measured at seven different heights from the ice surface: 1.0m, 2.0m, 3.0m, 3.5m, 4.0m, 4.5m, and 5.0 m, respectively. The air velocity was measured by using a digital hot wire anemometer. We recorded ten readings every 90 seconds, the ten readings were averaged to give the time-averaged air velocity. The typical standard error is 10 to 30 percent, where the standard error is defined as:

$$\text{s.e.} = \frac{1}{\bar{U}} \sqrt{\frac{1}{10} \sum_{i=1}^{10} (U_i(t) - \bar{U})^2} . \quad (7)$$

Figure 2 shows both experimental and numerical air velocity and temperature profiles at the six locations. The agreement between computed and measured temperature is good. However, there are discrepancies between the computed and measured velocity profiles. In such a large space, it is difficult to measure the velocity profile with a single anemometer. It took two days to complete the measurements. It is clear to see from the measured data that the velocity may not be the same because the velocity in the upper part of the arena (measured in the second day) is very different from that in the lower part (measured in the first day). Since the flow boundary condition at the inlet was measured in the first day, the agreement between the computed velocity and the measured data is much better in the first day. Due to the uncertainty in the measurements, the numerical results are acceptable.

CO concentration levels under steady state conditions

In order to evaluate the ability of the CFD model to predict the contaminant dispersal under steady state conditions a passive perfluorocarbon tracer gas (PFT) was used. This passive tracer gas method is presented in detail in another publication (Demokritou et al., 1999) Thirty PFT sources were distributed around the glass shielding of the ice arena at a height of 1.4 m, as shown on Figure 3. Tracer gas source characteristics are shown on Table 3. The HVAC system was operated continuously for 24 hours after the PFT sources were distributed in order to reach an equilibrium - steady state condition. Then absorption based passive samplers were deployed in selected locations (Figure 3) and remained in place for approximately an additional 48 hours. The samplers were located to measure the concentrations in a horizontal x-y plane at a 5.7 m height over the ice arena. The PFT vapor collected by the passive samplers was extracted in the laboratory and analyzed by a gas chromatography to determine the concentration levels.

The comparison of experimental and numerical concentration data are shown for various locations in the arena in Figure 4. The agreement between the computed and measured results is acceptable for the study of indoor air quality in ice rink arenas.

CO concentration levels during an ice-resurfacing cycle (transient conditions)

The validation has also been conducted in order to test the ability of the CFD technique to predict the concentration levels during and after an ice resurfacing cycle under transient conditions. Figure 5 shows the ventilation system and the building characteristics of the arena. The ventilation system consists of six inlets at ceiling height and two outlets located at both sides of the spectator's area. Each inlet is has an air supply area of 0.5m^2 while the size of each outlet is 1.0m^2 . The supplied airflow rate was measured and found to be $22,000\text{ m}^3/\text{hr}$.

An ice resurfacing cycle lasts approximately fifteen minutes. During ice resurfacing, the propane fueled ice resurfacers move in circles around the ice arena while the ventilation system is on all the time. In order to simulate the circular motion of the ice resurfacers, a number of contamination sources have been distributed over the ice surface. The contamination sources are activated sequentially for a period of time to simulate the movement of the resurfacers. (moving boundary source) as shown in Figure 5, where S_n stands the number of source. Table 2 shows the emission rate of each source and the duration time of activation. The average speed of the resurfacers is about 1.0 to 2.0 m/s and the distance between two CO sequential sources is 10 m.

CO concentration levels were measured at one minute intervals over approximately a 12 hour period on March 13th and a 5 hour period on March 16th, 1999. The instrument used was mounted 1.1 m above the ice surface at the center of the ice arena.

Figure 6 shows the experimental and simulated CO concentrations. The computed results are in good agreement with the experimental data. Note that the technique used to simulate the moving CO source is crucial to obtain the best numerical results. A uniform distribution of CO source on the ice surface cannot produce satisfactory results.

Discussion

The CFD model is a useful and economical tool to investigate how ventilation parameters such as air exchange rates, air distribution methods and control strategies affect the IAQ in ice rink arenas. The model can also be used to develop guidelines for ventilation system design.

Although the simulation process requires significant effort to input the building geometrical features and the boundary conditions, the personnel effort is much less than conducting actual measurements in an arena. The CFD results are much more informative. They contain detailed information such as contaminant concentrations, temperature, velocity, etc. at every location of an arena simulated. However, the measurements can only be done in a few locations. The flow and thermal boundary conditions in an arena are impossible to control and that leads to a great uncertainty in data quality.

The computing effort has become smaller and smaller due to the fast development in computer speed and capacity. For example, the transient simulations can be performed on a Pentium II, 400 MHz personal computer.

CONCLUSIONS

The paper presents the validation of a CFD model for the investigation of ventilation and IAQ in ice rink arenas. Validation tests included air velocity and temperature spatial distributions under steady-state conditions and contaminant dispersion under both steady-state and transient conditions. The contaminant is from the fossil powered resurfacing equipment. The results show that the CFD model is sufficiently good to predict the air velocity, air temperature, and contaminant concentrations in ice rink arenas. The CFD model is a powerful tool to study ventilation and indoor air quality in an ice rink. The validated CFD model will be used to develop engineering design guidelines for the ventilation system of such a built environment. The impact of fundamental ventilation parameters such as air exchange rate, air distribution methods and control strategies on IAQ will be numerically investigated .

ACKNOWLEDGMENT

The authors thank Mr. Shiping Hu, Mr. Jui-Chen R. Chang, and Ms. Beth A. Manoogian for their assistance in the field survey and experimental measurements. The project is sponsored jointly by Frank J. Zamboni & Co., Inc., New England Ice Skating Managers Association, the Ice Skating Institute, and Nova Scotia Sport and Recreation Commission.

REFERENCES

- Brauer, M. and Spengler, J.D. (1994) "Nitrogen dioxide exposures inside ice skating rinks," *Am. J. Publ. Health* 84: 429-433.
- CHAM (1998). "PHOENICS Version 3.1", CHAM Ltd, UK.
- Chen, Q., (1997). "Computational fluid dynamics for HVAC: success and failures", *ASHRAE Transactions*. 103(1), 178-187.
- Demokritou, P., Yang, C., Spengler, J.D. and Chen, Q. (1999) "An experimental method for contaminant dispersal characterization in large scale buildings for IAQ applications," Submitted to journal *Building & Environment*.
- Hangstrom, K.(1999)." The influence of heat and contaminant Source nonuniformity on the performance of three different room air distribution methods" *ASHRAE transactions 1999, vol. 105*.
- Int-Hout, D. and Kloostra, L. (1999) "Air distribution for large spaces," *ASHRAE Journal.*, 57-64. April.
- Launder, B.E. and Spalding, D.B. (1974). "The numerical computation of turbulent flows," *Computer Methods in Applied Mechanics and Energy*, 3, 269-289.
- Lee, K., Yangisawa, Y., Spengler, J.D., and Nakai, S. (1994) "Carbon monoxide and nitrogen dioxide levels in indoor ice skating rinks," *Journal of sports Science*. 12:279-283.
- Nielsen, P. (1994) "Prospects for computational fluid dynamics in room air contaminant control," *Proceedings of the 4th international Symposium on Ventilation for Contaminant control*, Stockholm.
- Patankar, S.V. (1980) *Numerical Heat Transfer and Fluid Flow*, New York, Hemisphere Publishing Corp.

Spengler, J.D., Stone, K.R., and Lilley, F. W. (1978). "High carbon monoxide levels measured in enclosed skating rinks," *Journal of Air Pollution. Control Association.* 28: 776-779.

Table 1: Values of Φ , $\Gamma_{\Phi,eff}$ and S_{Φ} for PDE equations.

| | Φ | $\Gamma_{\Phi,eff}$ | S_{Φ} |
|---|------------|-------------------------------------|--|
| Continuity | 1 | 0 | 0 |
| x-momentum | V_1 | $\mu + \mu_t$ | $-\partial P / \partial x$ |
| y-momentum | V_2 | $\mu + \mu_t$ | $-\partial P / \partial y$ |
| z-momentum | V_3 | $\mu + \mu_t$ | $-\partial P / \partial z - \rho g \beta (T - T_0)$ |
| T-equation | T | $\mu / \sigma_1 + \mu_t / \sigma_t$ | S_T |
| k-equation | k | $(\mu + \mu_t) / \sigma_k$ | $G - \rho \epsilon + G_B$ |
| ϵ -equation | ϵ | $(\mu + \mu_t) / \sigma_{\epsilon}$ | $[\epsilon (C_{\epsilon 1} G - C_{\epsilon 2} \rho \epsilon) / k] + C_{\epsilon 3} G_B (\epsilon / k)$ |
| Species | C | $(\mu + \mu_t) / \sigma_c$ | S_C |
| Age of air | τ | $\mu + \mu_t$ | ρ |
| $\mu_t = \rho C_{\mu} k^2 / \epsilon$ $G = \mu_t (\partial U_i / \partial x_j + \partial U_j / \partial x_i) \partial U_i / \partial x_j$ $G_B = -g (\beta / C_p) (\mu_t / \sigma_{T,t}) \partial T / \partial x_1$ | | | |
| $C_{\epsilon 1} = 1.44, C_{\epsilon 2} = 1.92, C_{\epsilon 3} = 1.44, C_{\mu} = 0.09$ $\sigma_t = 0.9, \sigma_k = 1.0, \sigma_{\epsilon} = 1.3, \sigma_C = 1.0$ | | | |

Table 2: Moving CO boundary source for transient state conditions.

| Time step | Time (s) | Source No. | Time step | Time (s) | Source No. |
|-----------|----------|------------|-----------|----------|------------|
| 1 | 0~10 | S1 | 16 | 150~160 | S16 |
| 2 | 10~20 | S2 | 17 | 160~170 | S17 |
| 3 | 20~30 | S3 | 18 | 170~180 | S18 |
| 4 | 30~40 | S4 | 19 | 180~190 | S19 |
| 5 | 40~50 | S5 | 20 | 190~200 | S20 |
| 6 | 50~60 | S6 | 21 | 200~210 | S21 |
| 7 | 60~70 | S7 | 22 | 210~220 | S22 |
| 8 | 70~80 | S8 | 23 | 220~230 | S23 |
| 9 | 80~90 | S9 | 24 | 230~240 | S24 |
| 10 | 90~100 | S10 | 25 | 240~250 | S25 |
| 11 | 100~110 | S11 | 26 | 250~260 | S26 |
| 12 | 110~120 | S12 | 27 | 260~270 | S27 |
| 13 | 120~130 | S13 | 28 | 270~280 | S28 |
| 14 | 130~140 | S14 | 29 | 280~290 | S29 |
| 15 | 140~150 | S15 | | | |

Table 3 : Tracer gas (PFT) source characteristics

| Source No. | Permeation Rate at 24°C (ng/min) | Permeation Rate at 9°C (ng/min) | Source No. | Permeation Rate at 24°C (ng/min) | Permeation Rate at 9°C (ng/min) |
|------------|----------------------------------|---------------------------------|------------|----------------------------------|---------------------------------|
| S1 | 1932.5 | 1062.9 | S16 | 1876.4 | 1032.0 |
| S2 | 1839.1 | 1011.5 | S17 | 1812.2 | 996.7 |
| S3 | 1803.7 | 992.0 | S18 | 1980.6 | 1089.3 |
| S4 | 1927.5 | 1060.1 | S19 | 1892.4 | 1040.8 |
| S5 | 1715.3 | 943.4 | S20 | 1874.4 | 1030.9 |
| S6 | 1741.8 | 958.0 | S21 | 1892.4 | 1040.8 |
| S7 | 1865.6 | 1026.1 | S22 | 1788.1 | 983.5 |
| S8 | 1913.4 | 1052.4 | S23 | 1750.7 | 962.9 |
| S9 | 1860.3 | 1023.3 | S24 | 1916.4 | 1054.0 |
| S10 | 1780.1 | 979.1 | S25 | 1780.1 | 979.1 |
| S11 | 1844.3 | 1014.4 | S26 | 1716.0 | 943.8 |
| S12 | 1996.6 | 1098.1 | S27 | 1796.2 | 987.9 |
| S13 | 2004.7 | 1102.6 | S28 | 1772.1 | 974.7 |
| S14 | 2060.1 | 1133.1 | S29 | 1956.5 | 1076.1 |
| S15 | 2051.3 | 1128.2 | S30 | 1828.2 | 1005.5 |

- a. Permeation rates were measured at 24 C.
- b. Temperature correction was based on 9 C source temperature.

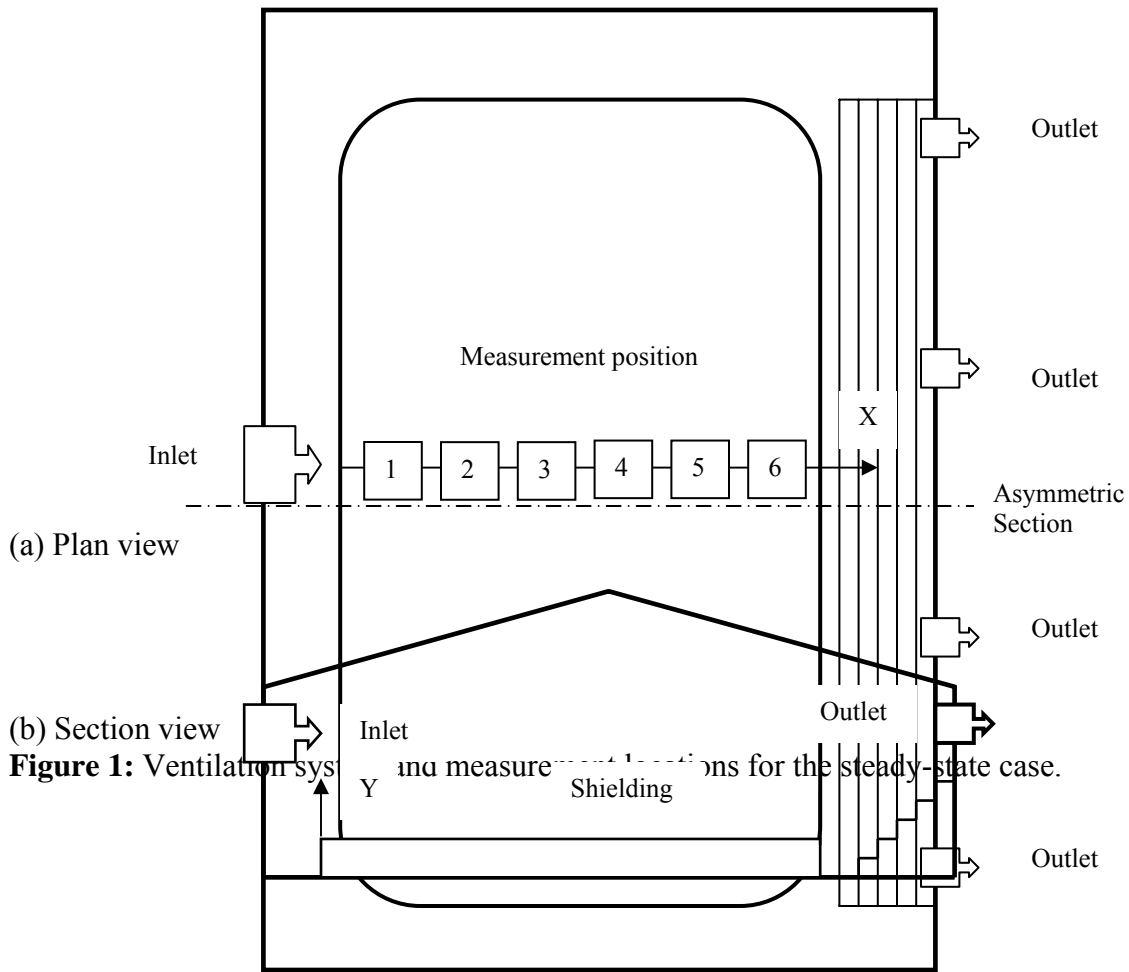
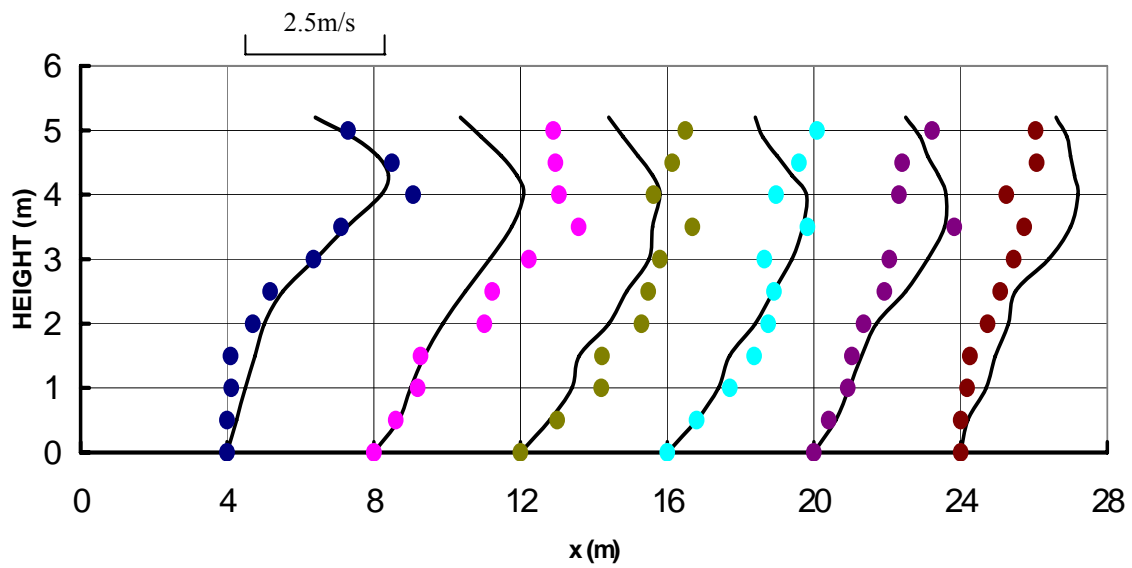
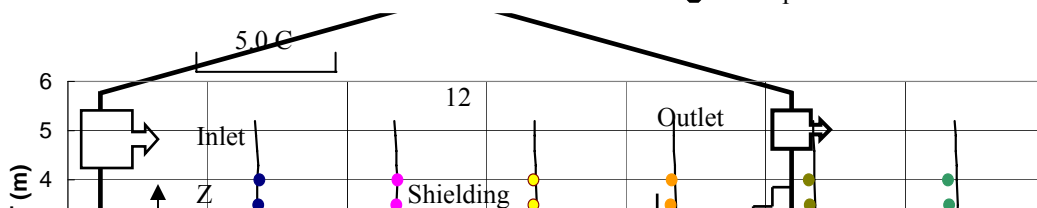


Figure 1: Ventilation system and measurement positions for the steady-state case.



(a) Velocity profiles

- Simulation
- Experimental



(b) Temperature profiles

Figure 2 Comparison of the computed and measured air velocity and temperature profiles for the steady-state case.

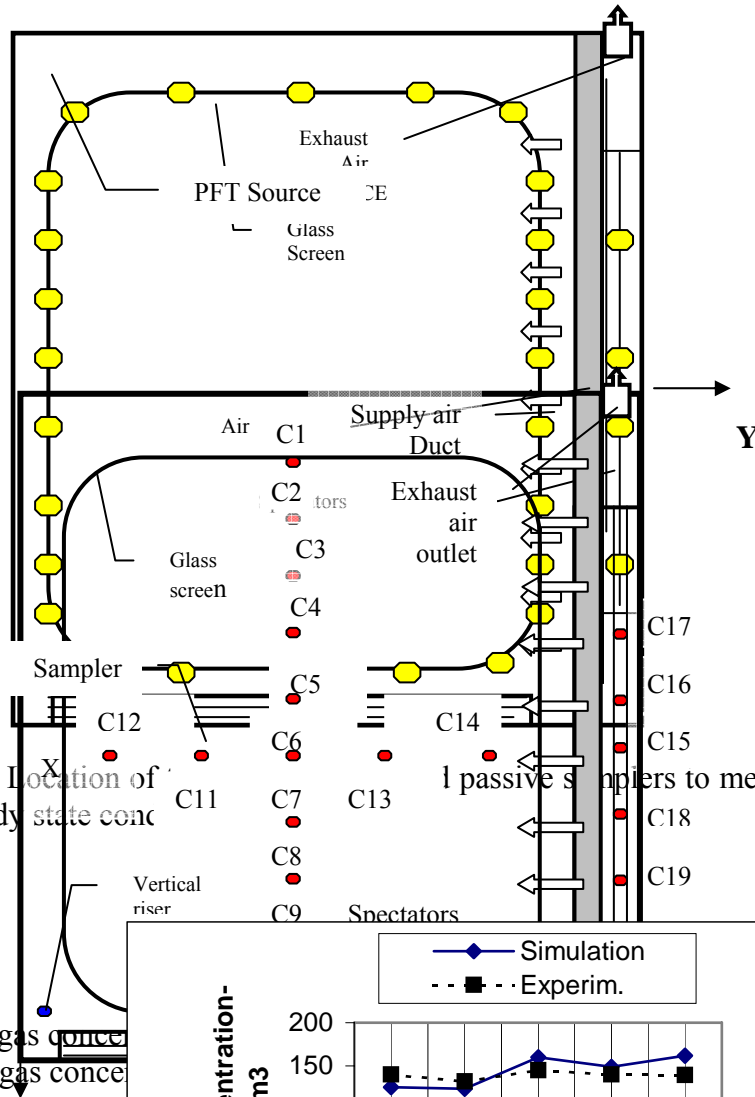


Figure 3: Location of under steady state conc

(a) Tracer gas conc
(b) Tracer gas conc

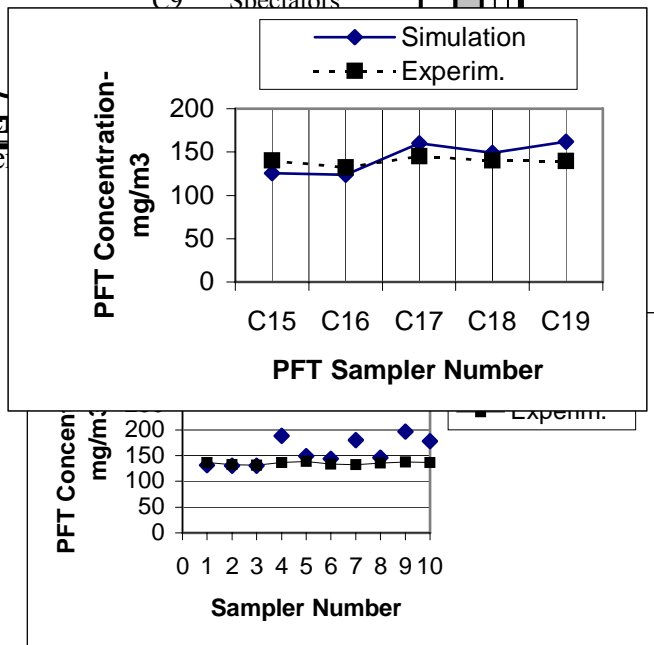


Figure 4: Experimental and numerical tracer gas concentrations under steady state conditions.

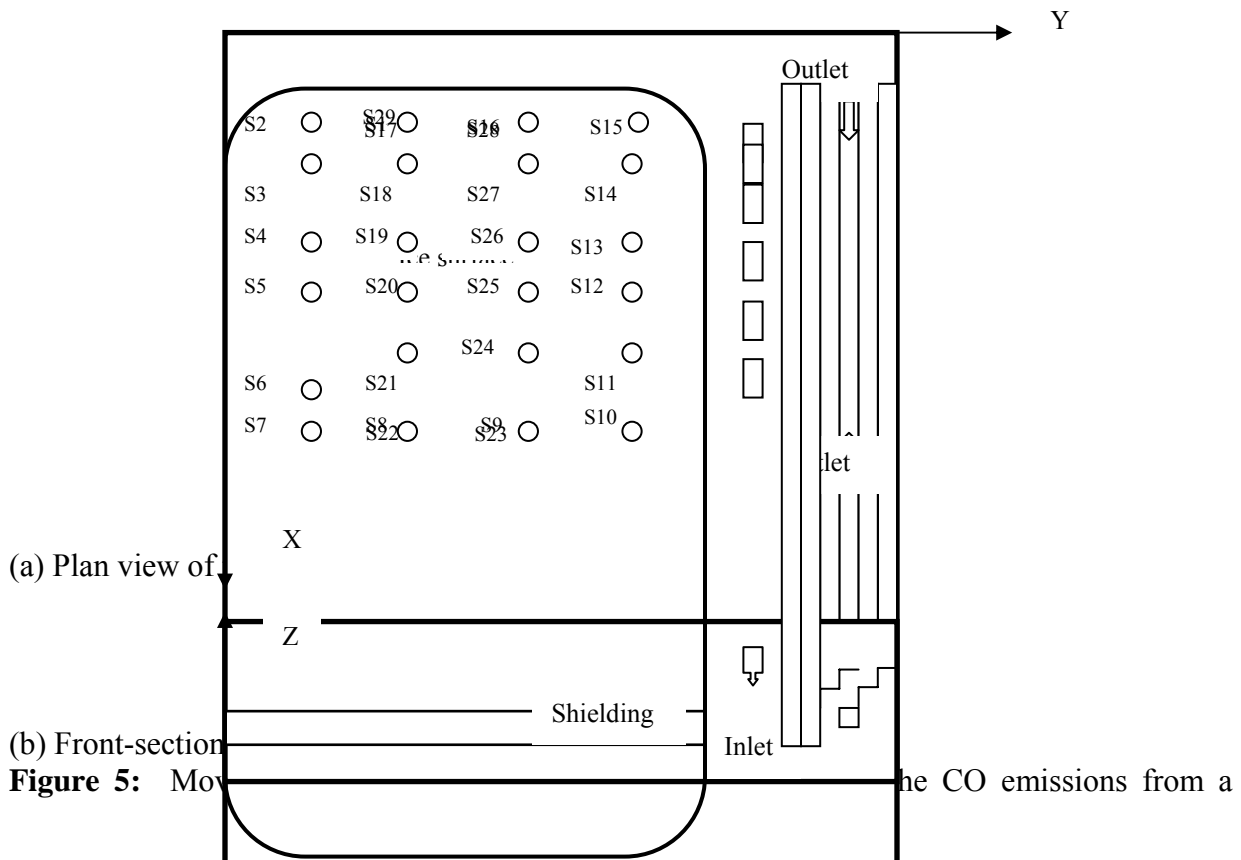
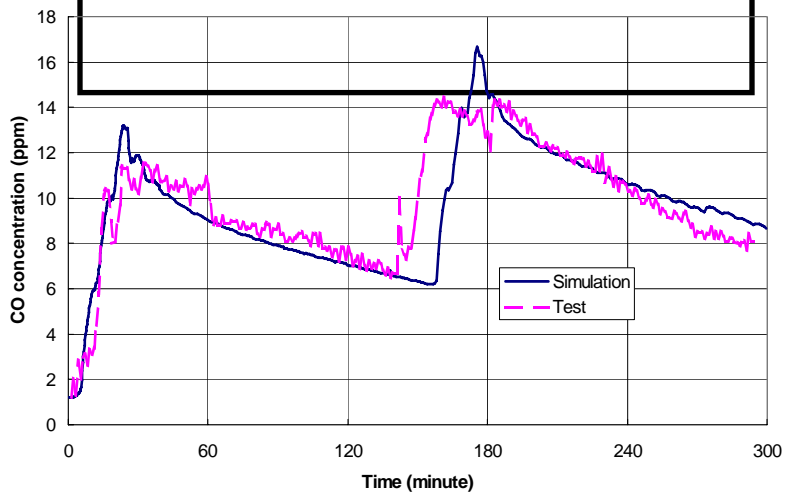


Figure 5: Movement of the CO emissions from a



resurfacer.

Figure 6: The measured and computed CO concentrations for transient conditions